



Structure and complexation mechanism of aqueous Zn(II)-acetate complex studied by XAFS and Raman spectroscopies

Alvaro Munoz-Noval^{1,2} · Kazuhiro Fukami³ · Takuya Kuruma^{2,4} · Shinjiro Hayakawa²

Received: 5 December 2023 / Accepted: 27 February 2024 / Published online: 5 April 2024
© The Author(s) 2024

Abstract

In this work, the structure of Zn acetate has been determined by a combination of X-ray absorption fine structure and Raman spectroscopy. We have analyzed the local atomic environment and the main vibrational bands of the acetate and Zn acetate at different pH. The results suggest that Zn acetate complex acquires a bidentate structure that modifies its first coordination shell. Meanwhile, the coordination shell of the hydrated Zn cation is formed by 6 hydroxides at a mean distance of 2.06 Å, the coordination shell of the Zn cation in the complex is formed by 2 hydroxides and 2 oxygens from the carboxyl group of the acetate, at a mean Zn–O distance of 1.96 Å. The structure of the Zn acetate complex is compared to those of Zn malonate and Zn citrate, none of which present a reduction in the coordination shell neither a shrinkage of the Zn–O shell distance.

Keywords Metal chelates · Structure of aqueous complexes · Raman spectroscopy · XAFS in liquids

Introduction

The use of chelating agents is nowadays broadly employed in industry for plating processes [1], heavy metal removal from soils, wastewaters and contaminated environments [2–5], etc. Particularly, in electrochemistry, the use of chelating agents has been successfully implanted for improving the metal deposition within nanoporous electrodes [6, 7]. The chelation of metals with carboxylic ligands allows tuning the size, the surface charge, and the solvation of the metal cation. All these physicochemical parameters are tightly involved in the occurrence of the surface-induced phase transition (SIFT) which causes accelerated mass transfer within nanopores under certain conditions.

In previous works, we have focused on studying which conditions determine SIFT when depositing Zn from Zn(II)-malonate and Zn(II)-citrate complexes [7]. To clarify the mechanism and the conditions required to happen, the relation between chelate structure and its performance in the SIFT, this work aims to study the Zn complex with acetic acid and compare it with more complex carboxylic acid complexes. In the carboxylates, the relation between structure and vibrational properties in acetate interacting with metal ions was studied by Nara et al. employing ab initio methods [8]. They found a relation among the relative frequencies of the vibrational modes of the symmetric (ν_s) and asymmetric (ν_a) stretching of the COO, and the difference of the frequencies, in cm^{-1} unit, was related to the spectrum with main structural parameters, such as the O–C–O angle (θ_{OCO}) and the relative asymmetry of the C–O bond lengths (δ_r):

$$\Delta_{s-a} = 1818.1\delta_r + 16.47(\theta_{\text{OCO}} - 120) + 66.8 \quad (1)$$

The Δ_{s-a} value for the ionic state (deprotonated acid) is employed as a reference for determining if a complex is bidentate (Δ_{s-a} lower than reference) or mono-dentate (Δ_{s-a} significantly larger than reference). This model has been in good agreement with experimental results for Ca [9, 10] or Mg [11] complexes. In the case of Zn, it has been extensively debated about the mono-dentate or bidentate interaction with the acetate ligand [12]. In this work, we have performed a

✉ Alvaro Munoz-Noval
alvaro.munoz.noval@ucm.es

¹ Department of Materials Physics, Faculty of Physics, University Complutense of Madrid, 28040 Madrid, Spain

² Department of Applied Chemistry, Graduate School of Engineering, Hiroshima University, Hiroshima 739-8527, Japan

³ Department of Materials Science and Engineering, Kyoto University, Kyoto 606-8501, Japan

⁴ Present Address: Mitsui Mining and Smelting Co Ltd, Shinagawa-Ku, Tokyo, Japan

detailed study of the Zn(II)-acetate complexation as a function of the pH, in order to understand the relation between the electrochemical performance of the complex with its structure, by a combined analysis using Raman and XAFS spectroscopies.

Zn complexes are critical in biological processes. Particularly, Zn(II)-acetate is a compound of medical interest [13]. As far as we know, its crystal structure was firstly studied in a di-hydrated, solid form by van Niekerk et al. [14] and later by Clegg et al. [15] and Ishioka et al. [16], using X-ray diffraction. In its solid form, they observed Zn adopts a distorted octahedral structure coordinated by two water O atoms and four acetate O atoms. However, up to our knowledge, the structure and coordination of the complex in its aqueous form has not been yet reported. In this regard, X-ray absorption fine structure (XAFS) spectroscopy, an element-selective, local probe technique that allows to characterize metal-organic compounds even in solution [17, 18] and determine with precision its local environment, including coordination, structure, and first-neighbor distances.

In this work, the structure and complexation of Zn(II)-acetate have been studied by XAFS and supported on Raman measurements to determine the pH-dependent complexation and structure. Finally, a comparative study of similar short-chain Zn(II)-carboxylates has permitted to get further insights into the coordination and structure of zinc carboxylates in an aqueous solution.

Experimental section

Materials

All the guaranteed reagents were used without further purification. Zinc sulfate heptahydrate ($\text{ZnSO}_4 \cdot 7\text{H}_2\text{O}$) was purchased from KISHIDA CHEMICAL Co., Ltd., Japan, and acetic acid (AA), malonic acid (MA), and citric acid (CA) were purchased from Nacalai Tesque, INC. Japan. Solutions were prepared by dissolving the reagents in ultra-pure water. Two types of mother solutions were prepared, and they contained one of the carboxylic acids (AA, MA, CA) and Zn of different molar ratios. One contained 1.0 M acetate (Ac) and 0.5 M Zn, and the other contained 2.0 M Ac and 0.5 M Zn. Solutions of different pH values were prepared by adding small volumes of commercial 1.0 M hydrochloric acid or sodium hydroxide.

Calculations of speciation curves

The Equilibrium speciation curves and fractional speciation diagrams for the aqueous Zn acetate system have been calculated with Visual Minteq software v.3.1 [19]. The equilibrium constants and Debye Hückel parameters included in the

Visual Minteq database have been employed for the calculations. Only major chemical species in the aqueous solution have been included for calculations. The speciation curves pKas and complex formation constants were calculated with the parameters listed in Table 1. The equilibrium fractional composition diagrams are calculated by determining a few chemical parameters (i.e. dissociation constants, etc.) and assuming thermodynamic relations. All the Zn species are in divalent cations. By increasing the pH the acetic acid is dissociated in ionic acetate and, in presence of the Zn(II) cation, the fraction of Zn(II)-acetate increases progressively in two species, Zn(II)-acetate⁺ or Zn(II)-acetate₂. It is predicted that the fraction of the Zn(II)-acetate₂ becomes dominant in the high pH region when the ratio of Ac/Zn is higher.

XAFS measurements

XAFS experiments at the Zn K-edge were carried out at BL01 and BL05 at SPring-8 (Hyogo, Japan) in transmission mode. The intensities of the incident and transmitted beams were monitored by ionization chambers filled with N₂ at atmospheric pressure. The liquid cell had two Kapton windows for the incident and transmitted beams, and the thickness of the cell was adjusted using an appropriate spacer for optimizing absorbance. The typical cell length was set to 3 mm. The spectra of 1.0 M ZnSO₄ and Zn(II)-acetate aqueous solutions at different pH conditions (i.e. 2, 3, 4, 4.5, 5, and 5.5) were acquired. Additional XAFS measurements in transmission mode were carried out in Zn(II)-malonate and Zn(II)-citrate at different pH: 2, 3, 4, 5 and 6 for Zn(II)-malonate and 1, 1.8, 3 and 4.8 for Zn(II)-citrate 1.0 M solutions.

XAFS data was reduced by employing the software pack Demeter by standard procedures [20]. To properly compare the XAFS spectra of the different solutions analyzed in this work, they were normalized using the same normalization procedure and setting the same normalization parameters. The pre-edge range was set from -200 eV to -30 eV respect to the edge, the normalization range from 110 to 780 eV respect to the edge, setting an order 3 of normalization [23]. EXAFS fittings were performed simultaneously in k and r-spaces employing theoretical paths from crystallographic references calculated with FEFF [21]. Best fits presented correspond to r-space, performed for k intervals from 1.8 to 10 Å⁻¹ weighted in k³ and r intervals of 1.2 to 3.3 Å.

Table 1 Dissociation constant of the carboxylic acids studied

Acid	Ligand (L)	pKa	References
Acetic acid (AA)	Acetate	4.76	[20]
Malonic acid (MA)	Malonate	2.83, 5.69	[21]
Citric acid (CA)	Citrate	3.09, 4.75, 5.41	[22]

The resolution limit for distinguishing two close shells by EXAFS is directly related to the maximum photoelectron wavenumber reached (that is, the kinetic energy of the photoelectron): $\delta R = \pi/2k_{\max}$. For the present work, on average the k_{\max} is 10 \AA^{-1} , meaning that two shells must be separated at least by ca. 0.16 \AA to be resolved. Ab initio calculations of the structures have been performed employing ab initio structures constructed employing CRYSTALFFREV [22] to obtain adequate FEFF input data files.

Raman measurements

Raman measurements were performed in a standard Raman spectrometer equipped with a single monochromator (T64000) and a diffraction grating (600 l/mm). The excitation source was an Ar⁺ laser ($\lambda = 514.5 \text{ nm}$) with an output power set to 400 mW. Several spectra were acquired for different sets of solutions for checking repeatability. The measured solutions in the Raman experiments were 0.1 M, 1.0 M, and 2.0 M CH₃COOH, (AcH) and 2.0 M Zn(II)-acetate, in the same range of pH as in the XAFS experiments. Raman spectra of water were acquired in every experimental session for subtracting the background of AcH and Zn(II)-acetate solutions taken under the same conditions.

Results and discussion

Raman spectra of the Zn complexes

In a previous paper, we investigated the complexation of Ca(II)-acetate, and the main bands in the vibrational spectra were identified for this complex based on the literature [10, 23–25]. To study the complexation of the cation, special attention was paid to carbonyl (C=O) and COO symmetrical and asymmetrical stretching vibrational modes ($\nu_s\text{COO}$ and $\nu_a\text{COO}$, respectively). The correlation between the intensity

of $\nu_s\text{COO}$ and C=O bands with the dissociation fraction of the carboxyl at different pH were also identified as useful signs for complexation. The intensity of the C=O band is linked to the protonated carboxyl (Ac-H) whereas the $\nu_s\text{COO}$ appears after the dissociation of the acid. The presence of the $\nu_s\text{COO}$ band is compatible with an ionic acetate complex or with a bidentate acetate-metal complex when there are metal cations in the solution. The Raman spectra and speciation curves for the solutions of 1.0 M acetic acid (AA) and solutions with ZnSO₄/AA 0.5/1.0 M, respectively, are included in Fig. 1 at the spectral region where the $\nu_s\text{COO}$ band appears (around 1408 cm^{-1}) for different pH. Figure 1a shows the Raman spectra in the region of the C=O, $\nu_a\text{COO}$ and $\nu_s\text{COO}$ bands for the 1.0 M Zn(II)-acetate and AA solutions in the range of pH of study. The spectra show a clear band intensity dependence with the pH in both solutions, AA and Zn/AA. As abovementioned, the relative $\nu_s\text{COO}$ band intensity ($\nu_s\text{COO}$ ratio) allows to semi-quantify the species concentration and compare with the theoretical speciation curves. In Fig. 1b, this $\nu_s\text{COO}$ ratio used as an indicator of the relative proportion of complexated Zn is compared with the speciation curves obtained numerically from thermodynamic calculations. The speciation curves considers two main Zn(II)-acetate species: once complexed Zn(II)-acetate and twice complexed Zn(II)-acetate (Zn(II)-acetate₂). The total concentration of Zn in form of Zn-complexes (as a sum of both species) in the calculated speciation curve does reach the Zn proportion (0.5 M) in solution because other Zn species in solution have not been included in the figure (see Figure S2 in the Supplementary Info).

The relative shift (Δ_{s-a}) measured in the Zn(II)-acetate solution at pH 5.5 provide values of about 154 cm^{-1} . To determine the character of the Zn(II)-acetate applying Nara's criteria, we obtain the Δ_{s-a} value for the ionic state of the acetate (deprotonated) as reference [8, 9] using the band intensity measured in the Raman spectra of Zn(II)-acetate solution at pH 5.5 (Figure S1). The experimental

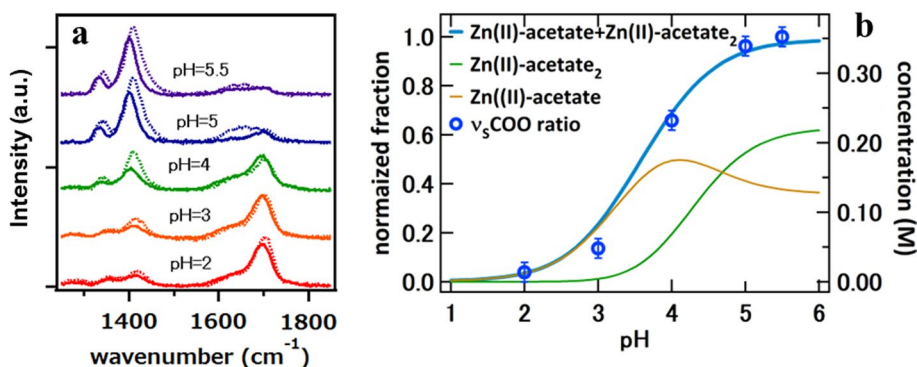


Fig. 1 Raman spectroscopy for the 1.0 M Zn(II)-acetate and AA solutions in the region of the C=O, $\nu_a\text{COO}$ and $\nu_s\text{COO}$ bands: **a** Zn(II)-acetate solutions (dashed lines) with pH ranging from 2 to 5.5 com-

pared to 1.0 M AA solutions (solid lines); **b** dissociation curve of the Zn(II)-acetate 0.5/1.0 M with the intensity ratio of the $\nu_s\text{COO}$ bands of the Zn(II)-acetate solution and AA solution with equal pH

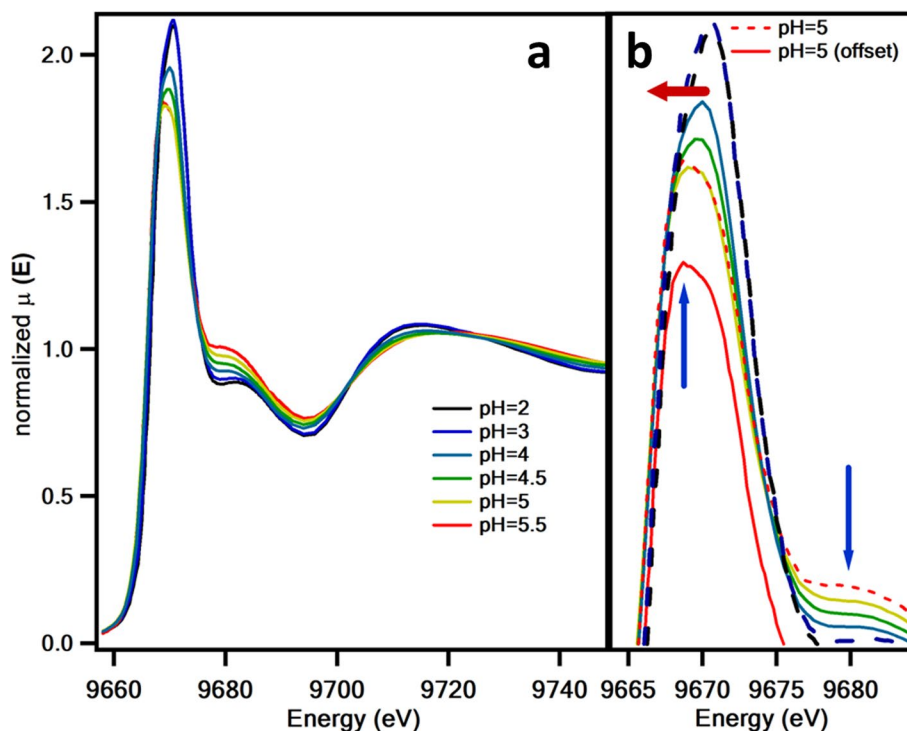
value for the Ac solution with pH 7 (not shown), mainly formed by dissociated acetate ($pK_a = 3.71$) is obtained from its corresponding Raman spectra, resulting on a value of 141.8 cm^{-1} . Thus, pointing to an ionic or weak bi-dentate character of the Zn(II)-acetate.

The Raman bands for the protonated acetate (Ac-H at 878 cm^{-1}) and the C–C symmetric stretching ($\nu_s \text{CC}$ at 915 cm^{-1}) are also sensitive to dissociation and complexation. The $\nu_s \text{CC}$ band is strongly coupled to the vibrational modes of the carboxyl and is employed to determine the complexated/non-complexated acetate in solution [10]. This band presents a band splitting for large cations¹⁰ but is not resolved in the case of Zn. Also, the Ac-H band is sensitive to acid dissociation previous works [26]. It is probably related to out-of-plane deformation of the OH in carboxylic groups. The relative intensities of these two bands are represented with the respective speciation curves of the dissociated acetate, protonated acetate, and Zn(II)-acetate species. Ac-H band and $\nu_s \text{CC}$ bands reproduce with high fidelity the slope of the speciation curve at both concentrations (Figure S3). Moreover, the normalized speciation curves of the ionic acetate and Zn(II)-acetate species present a gap which is roughly reproduced by the relative intensity of the $\nu_s \text{CC}$ band in the Zn/Ac solutions. Therefore, these two bands are quantitative indicators of the dissociation and complexation of the acetate.

XAFS analysis of zinc acetate in aqueous solutions

XAFS measurements of Zn solutions with acetic, malonic, and citric acids (Zn(II)-acetate, Zn(II)-malonate and Zn(II)-citrate solutions in the following) at different pH were performed at the Zn K-edge (9659 eV). In Fig. 2, the pH-dependent X-ray absorption near edge spectroscopy (XANES) spectra of the Zn(II)-acetate solutions are depicted. The intensity of the main peak clearly decreases with the increase of pH around the pK_a of acetic acid. The peak positions slightly shift to lower energies while the peak profile becomes asymmetric. Three isosbestic points, just before the main peak at about 9673 eV, 9710 eV, and 9725 eV, can be clearly distinguished and indicate the coexistence of two main species contributing to the spectra, presumably hydrated Zn and Zn(II)-acetate. The decrease in the intensity of the main peak with increasing pH upon pK_a may evidence the variation of the Zn–O bonding distance or the decrease of the electronegativity of the Zn–O bonding. Additionally, a charge transfer effect with the ligand caused by the covalency causes a slight energy shift for increasing pH [27, 28]. There is a noticeable asymmetry of the main peak at the highest pH, that is probably related to a change in the local symmetry of the Zn. The electronic configuration of Zn, with the 3d level filled ($3d^{10}4s^2$) is the cause of any change in the edge and pre-edge caused by the local symmetry of the cation would be subtle or practically unobservable [29].

Fig. 2 XANES spectra at the Zn K-edge of the Zn/Ac solutions with pH ranging from 2 to 5.5 **a**, showing details of the main peak in **b**



The Extended X-ray absorption fine structure (EXAFS) data of the Zn(II)-acetate solutions and their corresponding FT are included in Fig. 3 a and b, respectively. The main peak observed at about 2.06 Å (ca. 1.8 Å in the figure, there is no photoelectron phase correction) corresponds to the Zn–O first shell. A second region with a less intense signal between 2 and 4 Å is due to multiple scattering processes. The first coordination shell of the Zn in aqueous solutions is formed by 6 Oxygens from the hydration sphere

in octahedral coordination [30–32]. The multiple scattering signal is related to the multiple collisions of the photoelectron with the atoms in the proximities, including outer hydration shells, anions, etc. The multiple scattering signal shape changes noticeably when increasing pH conditions upon the pKa of the acetate (above pH 5). The EXAFS has been fitted to get the local structure parameters (Table 2). The EXAFS fitting model for the Zn(II)-acetate (Fig. 3c) is a structure with hydrated Zn ions in octahedral coordination.

Fig. 3 EXAFS spectra of the Zn(II)-acetate solutions: **a** raw EXAFS of the Zn(II)-acetate solutions with pH ranging between 2 and 5.5; **b** FT of the EXAFS data included in **a**; **c** FT of the EXAFS spectra and fittings of **b**

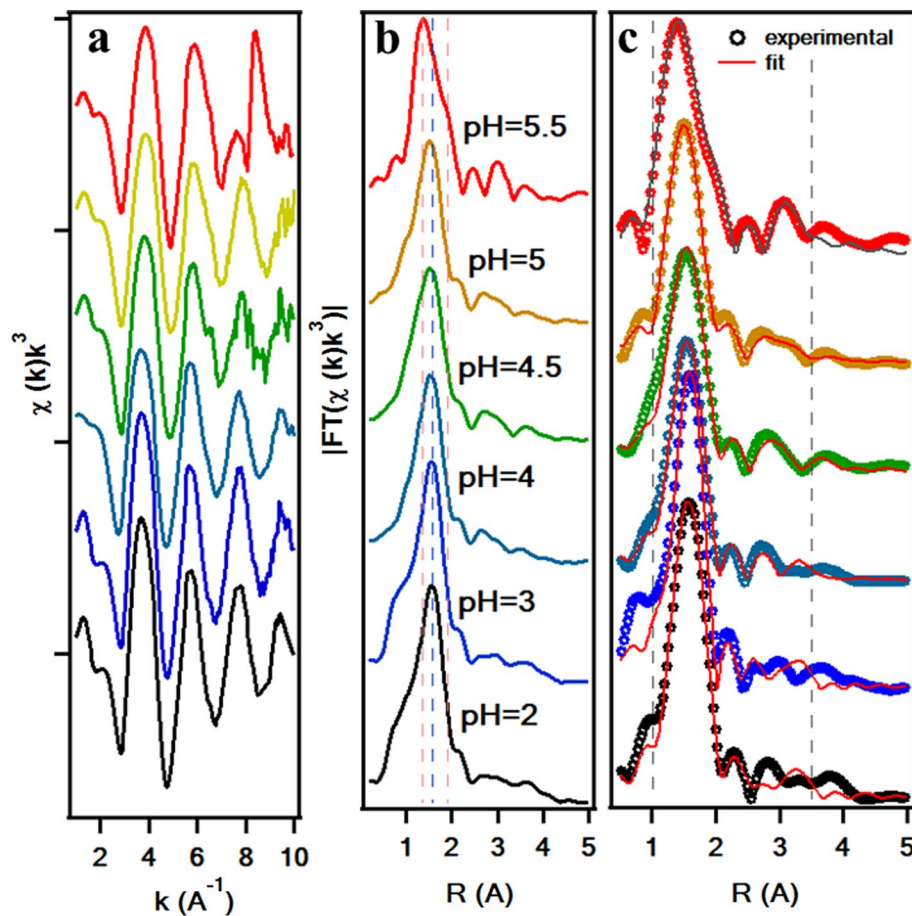


Table 2 Structural EXAFS parameters obtained from the fittings in the Zn(II)-acetate solutions

	pH EXAFS	2	3	4	4.5	5	5.5
O	N (O)	6.0 (5)	6.7 (5)	6.3 (5)	6.7 (5)	5.9 (5)	4.2 (5) 2.4 (5)
	R(Zn-O1)	2.08 (1)	2.05 (2)	2.06 (2)	2.04 (2)	2.02 (2)	1.96 (2)
	R(Zn-O2)				–	–	2.74 (2)
	σ^2 (O1)	0.011 (2)	0.012 (1)	0.010 (2)	0.012 (2)	0.011 (1)	0.0033 (7)
	σ^2 (O2)						0.0133 (8)
	σ^2 (MS)	0.012 (1)	0.018 (3)	0.017 (2)	0.015 (3)	0.009 (2)	0.015 (2)
	E	2 (1)	5 (1)	4 (1)	6 (1)	5 (1)	7 (1)
	R-coef	0.010	0.011	0.004	0.005	0.003	0.005
	χ^2	100	166	210	302	156	170

Remarkably, the Zn–O shell shifts to lower distances, of about 0.1 Å in the case of pH above the pKa, and the best fit is obtained with a first coordination shell of 4.2(5) oxygens at 1.96(2) Å including a second coordination Zn–O shell with average coordination of 2.4 (5) at 2.74(2) Å (Table 2).

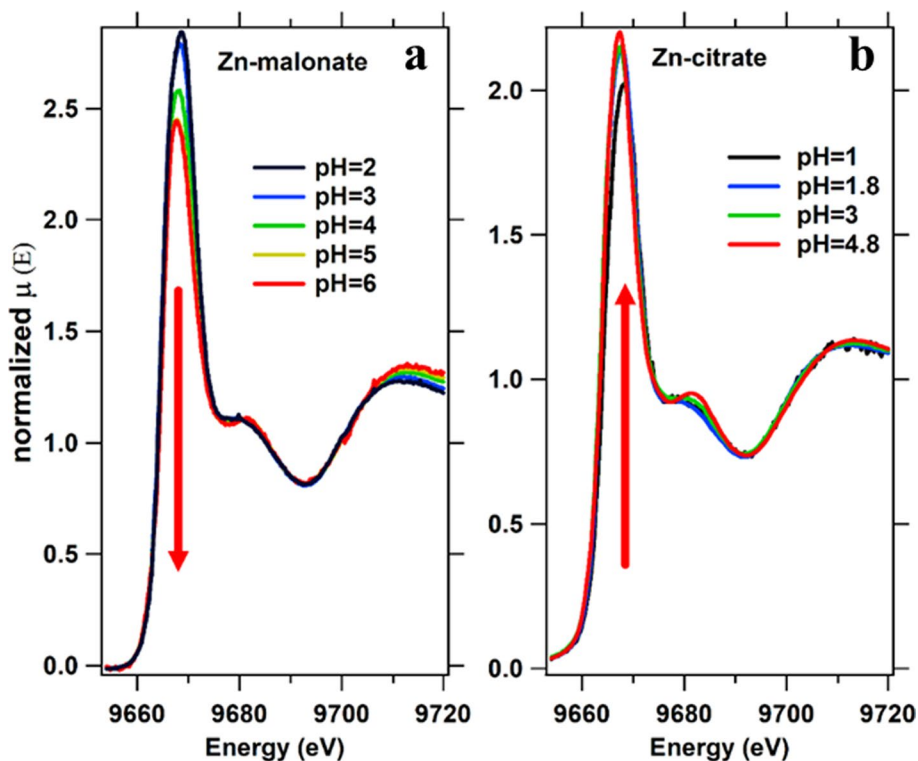
A comparative XAFS study of zinc carboxylates

To further understand the complexation mechanism and the complex structure, similar experiments have been conducted on Zn solutions with malonate and citrate salts (Zn(II)-malonate and Zn(II)-citrate, respectively) at different pH within the range of the first and second pKa [7]. In Fig. 4, the XANES spectra of both groups of solutions at different pH are shown. The intensity of the main peak of the Zn(II)-malonate solutions spectra decreases with increasing pH as there is a slight shift of the main peak center to lower energies. These two features were observed also for the Zn(II)-acetate solutions upon pH increase, as well as an increase of the second resonance intensity and deformation of the main peak shape at pH above pKa. In the case of Zn(II)-malonate solutions, the trend is equivalent at pH > 4, and the spectra do not change for pH 5 and pH 6. In the group of Zn(II)-citrate, solutions the effect of pH in the main peak intensity is the opposite, as it increases with pH. The decrease of the Zn–O covalent bonding upon complexation with malonate could explain similar behavior of the XANES main peak in Zn(II)-acetate, as the lowest peak intensity is observed at

pH 4 (first pKa of the malonic acid). The evolution of the spectra with pH for the Zn(II)-citrate solutions behaves the opposite the main peak intensity increases with pH, indicating an increase in the Zn–O bonding.

The FTs of the EXAFS spectra in the Mal(Cit)/Zn solutions at different pH are summarized in Fig. 5. The FTs of the EXAFS signal show similar features in the three Zn complexes (Ac/Mal/Cit): the main peak at ca. 2 Å and a multiple scattering signal above 2.5 Å. A change in the MS region at pH above the respective pKa is observed in the three groups of solutions, coinciding with complex formation. The fittings results of the EXAFS spectra of each complex at the pH > pKa condition are summarized in Table 3. There are two main differences between the FT of the EXAFS of the three Zn complexes. First, in the average coordination of the first atomic shell and second, in the first shell distance. Meanwhile, in Zn(II)-acetate and Zn(II)-malonate the first shell is on average formed by 4–5 oxygen atoms, in the Zn(II)-citrate the average number of atoms in the shell is almost 6, as in the case of hydrated Zn(II). The Zn–O shell distance in the Zn(II)-citrate is considerably larger than for the Zn(II)-acetate and Zn(II)-malonate (1.96 Å), and closer to the Zn(II) in solutions (2.06 Å), in opposition to the Zn(II)-acetate and Zn(II)-citrate. The interplay of both parameters, average shell coordination, and distance, would be related to the observed evolution in the XANES spectra. In the case of Zn(II)-acetate/Zn(II)-malonate, there is a diminishing in the main peak intensity, competing with a

Fig. 4 XANES of the Zn(II)-malonate and Zn(II)-citrate: spectra at the Zn K-edge of the **a** Zn(II)-malonate solutions with pH ranging from 2 to 6 and **b** Zn(II)-citrate ranging from pH 1 to 4.8



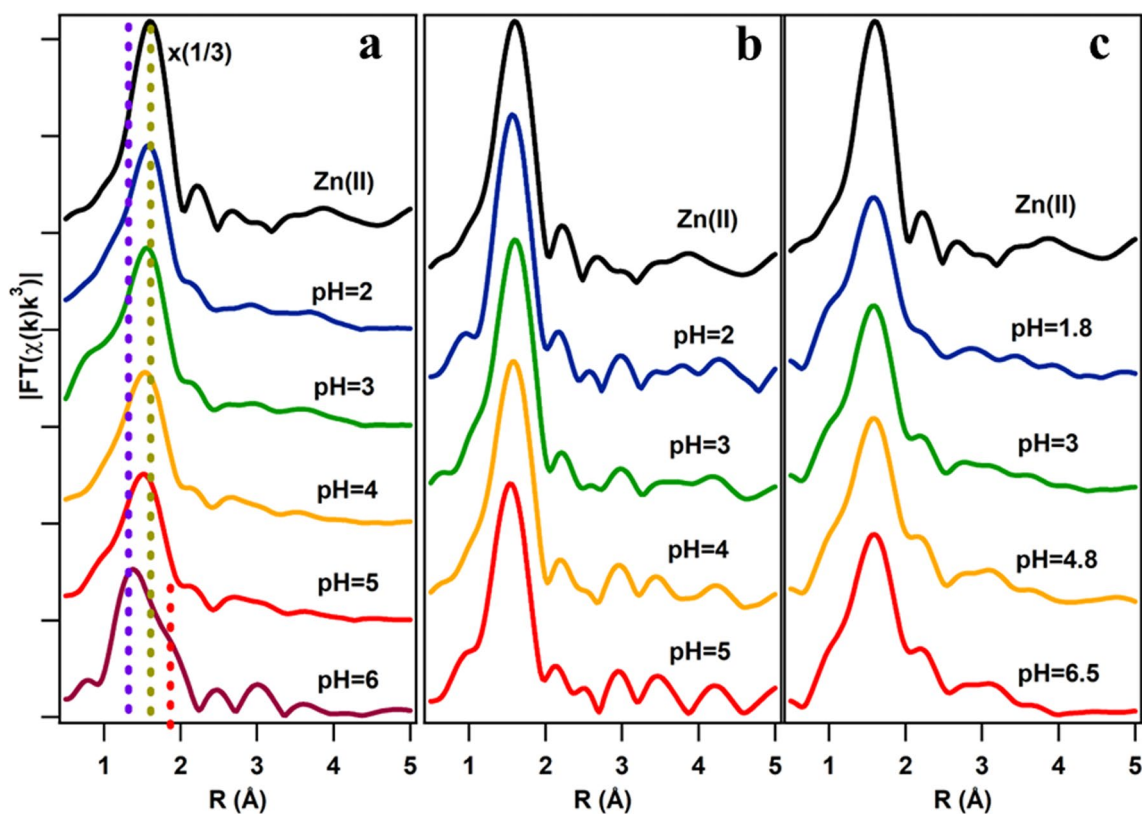


Fig. 5 FT of the EXAFS of the Zn carboxylate solutions: **a** Zn(II)-acetate, **b** Zn(II)-malonate and **c** Zn(II)-citrate at different pH conditions. The FT intensity of the Zn(II) solution in **a** is multiplied by a

factor 1/3 to be compared with the spectra of Zn(II)-acetate solutions. In **a**, the dashed lines help the reader to identify the evolution of the main features of the EXAFS signal with increasing pH

Table 3 EXAFS parameters of the best fit in the Zn(II) aqueous solution of the different complex studied

Zn(II)-	1st Zn–O shell			2nd Zn–O shell		
	N	R(Å)	DW	N	R	DW
Hydrated	6.0 (5)	2.06 (2)	0.011 (1)			
Acetate	4.2 (5)	1.96 (2)	0.0033 (5)	2.4 (5)	2.74 (2)	0.013 (2)
Malonate	4.8 (5)	1.96 (2)	0.014 (1)			
Citrate	5.9 (5)	2.02 (2)	0.013 (1)			

shell radius decrease that by itself would lead to an increase of the main peak intensity. However, the interplay of these two parameters and the decrease in the coordination of the first shell, observed by EXAFS, may result in the observed XANES features. The opposite reasoning would apply for Zn(II)-citrate because the shell coordination and radius are very close to the hydrated Zn, the peak intensity increase should be related to an increase in the covalency of the Zn binding.

At pH 5.5, the coordination of the Zn–O shell distance contracts to 1.96 Å, and its coordination decreases to 4. The best fit is performed including a second shell (Zn–O) with average coordination 2 at 2.74 Å. Considering the Raman data, the most plausible structure of the Zn(II)-acetate

complex is a weak bidentate (some authors use the term ionic) structure where the hydration sphere consists of a 4 O and the acetate O is placed at a second shell [33]. Several authors [16, 34] have found evidence that Zn(II)-acetate does not follow Nara criteria when has a chelating structure or low symmetry bridging or monodentate. However, following Ishioka, the rocking modes in the spectra may contain additional clues on the character and structure of the complex. We have preliminary compared the O–C–O out-of-plane rocking modes of the acetate upon dissociation with the corresponding to the complexation with Zn cations. The data presented as supplementary information (Figure S4), can be compared to the spectra measured in equivalent Ca(II)-acetate solutions [10], showing noticeable

differences. For instance, the rocking band in the Zn(II)-acetate shifts clearly to lower frequencies as the dissociated species ratio increases (about 30 cm^{-1}). A similar behavior has been observed for the Ca(II)-acetate [10], but presenting larger shift (above 50 cm^{-1}). Such a change in the mode frequency is compatible with a change in the spring force.

The Zn(II)-acetate spectrum shows a more complex behavior, being the band split in two above the pKa and its intensity noticeably damped with respect to the bidentate Ca(II)-acetate and ionic species [35–41]. These Raman spectral features and the EXAFS results may be compatible with the formation of the Zn(II)-acetate₂ complex at enough high pH conditions. From our experience, such Zn(II)-acetate₂ complexation is possible and relatively stable. In such structure, the first coordination shell may be formed by Zn–O of the acetate group and the second by the solvation sphere. We have observed similar behaviour in other Cu(II)-lactate complexes in alkaline solutions [42]. In this work, the complexation of Cu²⁺ with lactate showed a very slow complexation. This means that the fraction of the species may change with time after preparation and the deviation is prominent just near the neutralization point at an alkaline side. This suggests that in the Zn(II)-acetate solutions near pH 5 the fraction of the species in the solution may fluctuate, even in equivalently-aged samples. For the EXAFS experiments, we worked with relatively fresh samples, prepared with few hours in advance (we fabricated Zn/AA solutions of a maximum pH 6, but even at these pH values, we did not observe any precipitation). For enough large reaction times after sample preparation, the EXAFS at pH 5 may present signatures of Zn(II)-acetate₂ formation, but it would be the subject of a future work on the complex titration and complexation kinetics.

In Zn(II)-malonate and Zn(II)-citrate complexes the best fit is always given for a unique Zn–O shell. Therefore, the hydration shell and the O's of the carboxylate are at the same distance from the Zn(II) cation, at around 1.96 and 2.02 Å, respectively. The coordination number of the first shell in both cases is noticeably lower than that of the hydrated Zn(II) being compatible with the contraction observed in the shell distances. In opposition to Zn(II)-acetate, in both cases, in the range of pH studied in this work, there are not signatures of complexed species other than Zn(II)-malonate and Zn(II)-citrate, in their respective solutions.

Conclusions

The pH-dependent speciation and the structure of the Zn(II)-acetate complex have been studied in an aqueous medium by combining Raman and XAFS spectroscopy. The modification of the vibrational modes of the carboxyl ligand through the complexation with Zn(II) indicates the Zn(II)-acetate

complex has weak bidentate coordination in solution. The $\nu\text{C-C}$ and Ac-H bands have shown to be sensitive not only to acetic acid dissociation but also can differentiate the Zn complexed from the non-complexed acetate species. The XAFS shows clear structural differences in the Zn(II)-acetate with respect to the hydrated Zn(II). The measured coordination of the Zn(II)-acetate is close to 4 and the shell distance contracts by about 0.1 Å with respect to the hydrated Zn(II), presenting evidences of the formation of Zn(II)-acetate₂ complex at pH 5.5. In such case, the oxygens of the carboxyl would occupy the first coordination shell and the solvation shell is probably expanded to 2.74 Å. However, the determination of the Zn(II)-acetate, malonate and citrate complexes structure and stability requires further investigation and numerical calculations.

Supplementary Information The online version contains supplementary material available at <https://doi.org/10.1007/s44211-024-00549-z>.

Acknowledgements A.M.N. acknowledges Comunidad de Madrid and Universidad Complutense de Madrid for the project 2018-T1/IND-10360 granted by “Atracción de Talento” program and the Ministerio de Ciencia e Innovación for the grant PID2021-126323OA-I00. This study was also supported by JSPS Grant-in-Aid for Scientific Research B (Grant Number 21H01670; K.F.).

Funding Open Access funding provided thanks to the CRUE-CSIC agreement with Springer Nature.

Data availability Data will be made available upon reasonable request.

Declarations

Conflict of interest Authors declare there are not conflict of interests.

Open Access This article is licensed under a Creative Commons Attribution 4.0 International License, which permits use, sharing, adaptation, distribution and reproduction in any medium or format, as long as you give appropriate credit to the original author(s) and the source, provide a link to the Creative Commons licence, and indicate if changes were made. The images or other third party material in this article are included in the article's Creative Commons licence, unless indicated otherwise in a credit line to the material. If material is not included in the article's Creative Commons licence and your intended use is not permitted by statutory regulation or exceeds the permitted use, you will need to obtain permission directly from the copyright holder. To view a copy of this licence, visit <http://creativecommons.org/licenses/by/4.0/>.

References

1. Y.M. Lin, S.C. Yen, Effects of additives and chelating agents on electroless copper plating. *Appl. Surf. Sci.* **178**, 116–126 (2001)
2. F. Fu, Q. Wang, Removal of heavy metal ions from wastewaters: a review. *J Environ. Manag.* **92**, 407–418 (2011)
3. R.W. Peters, L. Shem. Chapter 6. *Use of chelating agents for remediation of heavy metal contaminated soil*. ACS Symposium Series. eISBN: 9780841213654. October 27, (1992), pp. 70–84
4. D. Leštan, C.L. Luo, X.D. Li, The use of chelating agents in the remediation of metal-contaminated soils: a review. *Environ. Pollut.* **153**, 3–13 (2008)

5. J.A. Entry, N.C. Vance, M.A. Hamilton, D. Zabowski, L.S. Watrud, D.C. Adriano, Phytoremediation of soil contaminated with low concentrations of radionuclides. *Water Air Soil Pollut. Pollut.* **8**, 167–176 (1996)
6. A. Koyama, K. Fukami, Y. Suzuki, A. Kitada, T. Sakka, T. Abe, K. Murase, M. Kinoshita, High-rate charging of zinc anodes achieved by tuning hydration properties of zinc complexes in water confined within nanopores. *J. Phys. Chem. C* **120**, 24112–24120 (2016)
7. A. Muñoz-Noval, K. Fukami, A. Koyama, T. Kuruma, A. Kitada, K. Murase, T. Abe, T. Sakka, S. Hayakawa, Mechanism of accelerated zinc electrodeposition in confined nanopores, revealed by X-ray absorption fine structure spectroscopy. *J. Phys. Chem. C* **121**, 18047–18056 (2017)
8. M. Nara, H. Torii, M. Tasumi, Correlation between the vibrational frequencies of the carboxylate group and the types of its coordination to a metal ion: an ab initio molecular orbital study. *J. Phys. Chem.* **100**, 19812–19817 (1996)
9. A.S. Milev, G.S.K. Kannangara, M.A. Wilson, Template-directed synthesis of hydroxyapatite from a lamellar phosphonate precursor. *Langmuir* **20**, 1888–1894 (2004)
10. A. Muñoz-Noval, D. Nishio, T. Kuruma, S. Hayakawa, Coordination and structure of Ca (II)-acetate complexes in aqueous solution studied by a combination of Raman and XAFS spectroscopies. *J. Mol. Struct. Mol. Struct.* **1161**, 512–518 (2018)
11. H. Nickolov, I. Ivanov, G. Georgiev, D. Stoilova, Raman study of complexation in aqueous solutions of magnesium acetate. *J. Mol. Struct.* **377**, 13–17 (1996)
12. M.M. Yang, D.A. Crerar, D.E. Irish, A Raman spectroscopic study of lead and zinc acetate complexes in hydrothermal solutions. *Geochim. Cosmochim. Acta. Cosmochim. Acta* **53**, 319–326 (1988)
13. L.A. Anderson, S.L. Hakojarvi, S.K. Boudreaux, Zinc acetate treatment in Wilson's disease. *Ann. Pharmacother. Pharmacother.* **32**, 78–87 (1998). <https://doi.org/10.1345/aph.17075>
14. J.N. van Niekerk, F.R.L. Schoening, Talbot. *Acta Cryst.* **6**, 720–723 (1953)
15. W. Clegg, I.R. Little, Straughan. *Acta Cryst.* **C42**, 1701–1703 (1986)
16. T. Ishioka, A. Murata, Y. Kitagawa, K.T. Nakamura, Zinc (II) acetate dihydrate. *Acta Cryst.* **C53**, 1029–1031 (1997)
17. O. Alexeev, B.C. Gates, EXAFS characterization of supported metal-complex and metal-cluster catalysts made from organometallic precursors. *Top. Catal. Catal.* **10**, 273–293 (2000)
18. L. Wentian, H.H. Thorp, Bond valence sum analysis of metal-ligand bond lengths in metalloenzymes and model complexes. 2. Refined distances and other enzymes. *Inorg. Chem. Chem.* **32**, 4102–4105 (1993)
19. J.P. Gustafsson Visual MINTEQ (v3.0). A Windows version of MINTEQA2 (2012), <http://vminteq.lwr.kth.se/>
20. B. Ravel, M. Newville, ATHENA, ARTEMIS, HEPHAESTUS: data analysis for X-ray absorption spectroscopy using IFEFFIT. *J. Synchrotron. Rad.* **12**, 537 (2005)
21. A.L. Ankudinov, B. Ravel, J.J. Rehr, S.D. Conradson, Real-space multiple-scattering calculation and interpretation of x-ray-absorption near-edge structure. *Phys. Rev. B* **58**, 7565 (1998)
22. A. Michalowicz, J. Moscovici, D. Bouvet-Muller, K. Provost, MAX (multiplatform applications for XAFS) new features. *J. Phys. Conf. Ser.* **430**, 112016 (2013)
23. F. Quiles, A. Burneau, Infrared and Raman spectra of alkaline-earth and copper (II) acetates in aqueous solutions. *Vib. Spectrosc. Spectrosc.* **16**, 105–117 (1998)
24. P. Persson, M. Karlsson, L.O. Ohman, Coordination of acetate to Al(III) in aqueous solution and at the water-aluminum hydroxide interface: a potentiometric and attenuated total reflectance FTIR study. *Geochim. Cosmochim. Acta. Cosmochim. Acta* **62**, 3657–3668 (1998)
25. V. Zelenak, Z. Vargova, K. Gyoryova, Correlation of infrared spectra of zinc (II) carboxylates with their structures. *Spectrochim. Acta Part A.* **66**, 262–272 (2007)
26. J.T.L. Navarrete, V. Hernandez, F.J. Ramirez, Vibrational study of aspartic acid and glutamic acid dipeptides. *J. Mol. Struct. Struct.* **348**, 249 (1995)
27. P.G. Jones, J.J. Guy, G.M. Sheldrick, Bis (ethylenethiourea) gold (I) chloride hydrate. *Acta Cryst.* **B32**, 3321–3322 (1976)
28. E.A. Stem, S.M. Heald, X-ray filter assembly for fluorescence measurements of x-ray absorption fine structure. *Rev. Sci. Instr.* **50**, 1579 (1979)
29. T. Yamamoto, Assignment of pre-edge peaks in K-edge x-ray absorption spectra of 3d transition metal compounds: electric dipole or quadrupole? *X-Ray Spectrom. Spectrom.* **37**, 572–584 (2008)
30. P. Frank, M. Benfatto, R.K. Szilagy, P. D'Angelo, S. Della Longa, K.O. Hodgson, The solution structure of [Cu(aq)]²⁺ and its implications for rack-induced bonding in blue copper protein active sites. *Inorg. Chem. Chem.* **44**, 1922–1933 (2005)
31. P. D'Angelo, M. Benfatto, S. Della Longa, N.V. Pavel, Combined XANES and EXAFS analysis of Co²⁺, Ni²⁺ and Zn²⁺ aqueous solutions. *Phys. Rev. B* **66**, 064209 (2002)
32. *Structure and dynamics of solutions*, eds: H. Ohtaki, H. Yamatera. (Elsvier, 1992). eBook ISBN: 9781483291420
33. H.G.M. Edwards, I.R. Lewis, Vibrational spectroscopic studies of iron (II) acetate. *J. Mol. Struct. Struct.* **296**, 20 (1993)
34. V. Zelenak, Z. Vargova, K. Gyoryova, Correlation of infrared spectra of zinc (II) carboxylates with their structures. *Spectrochim Acta Part A Mol. Biomol. Struct.* **66**, 262–272 (2007)
35. H. Ohtaki, T. Radnai, Structure and dynamics of hydrated ions. *Chem. Rev.* **93**, 1157 (1993)
36. R.E. Kruh, C.L. Standley, An X-ray diffraction study of aqueous zinc chloride solutions. *Inorg. Chem. Chem.* **1**, 941 (1962)
37. D.L. Wertz, J.R. Bell, On the existence of pseudo-tetrahedral tetrachlorozincate (II) in hydrochloric acid solutions. *J. Inorg. Nucl. Chem. Inorg. Nucl. Chem.* **35**, 137 (1973)
38. G. Paschina, G. Piccaluga, G. Pinna, M. Magini, Chloro-complexes formation in a ZnCl₂-CdCl₂ aqueous solution: an x-ray diffraction study. *J. Chem. Phys.* **78**, 5745 (1983)
39. P. Dreier, P. Raber, EXAFS-study of the Zn²⁺ coordination in aqueous halide solutions. *J. Phys. Colloques.* **47**, 809–812 (1986)
40. T. Yamaguchi, S. Hayashi, H. Ohtaki, X-ray diffraction and Raman studies of zinc (II) chloride hydrate melts, ZnCl₂·rH₂O (r= 1.8, 2.5, 3.0, 4.0, and 6.2). *J. Phys. Chem.* **93**, 2620 (1989)
41. D.H. Powell, P.M.N. Gullidge, G.W. Neilson, Zn²⁺ hydration and complexation in aqueous electrolyte solutions. *Mol. Phys.* **71**, 1107 (1990)
42. T. Chen, A. Kitada, Y. Seki, K. Fukami, D.T. Usmanov, L. Chuin Chen, K. Hiraoka, K. Murase, Identification of copper(II)-lactate complexes in Cu₂O electrodeposition baths: deprotonation of the α-hydroxyl group in highly concentrated alkaline solution. *J. Electrochem. Soc. Electrochem. Soc.* **165**, D4444–D4451 (2018)